

Received: 2018.11.20

Accepted: 2019.01.22

Published: 2019.05.11

Diagnostic Performance of Perfusion Computed Tomography for Differentiating Lung Cancer from Benign Lesions: A Meta-Analysis

Authors' Contribution:

Study Design A
Data Collection B
Statistical Analysis C
Data Interpretation D
Manuscript Preparation E
Literature Search F
Funds Collection G

DE 1,2 **Cuiqing Huang***

BF 1 **Jianye Liang***

DF 3 **Xueping Lei**

B 1 **Xi Xu**

AC 1 **Zeyu Xiao**

A 1 **Liangping Luo**

1 Medical Imaging Center, The First Affiliated Hospital of Jinan University, Guangzhou, Guangdong, P.R. China

2 Department of Ultrasound, Guangdong Women's and Children's Hospital, Guangzhou, Guangdong, P.R. China

3 Key Laboratory of Molecular Target and Clinical Pharmacology, School of Pharmaceutical Sciences and Fifth Affiliated Hospital, Guangzhou Medical University, Guangzhou, Guangdong, P.R. China

* Cuiqing Huang and Jianye Liang contributed equally to this work

Corresponding Authors: Liangping Luo, e-mail: tluolp@jnu.edu.cn, Zeyu Xiao, e-mail: zeyuxiao@jnu.edu.cn

Source of support: Departmental sources

Background: Numerous studies have explored diagnosis of pulmonary nodules using perfusion computed tomography (CT); however, findings were not always consistent between studies. The present study aimed to summarize evidence on the diagnostic value of perfusion CT for distinguishing between lung cancer and benign lesions.

Material/Methods: We performed a systematic literature search on lung cancer and benign pulmonary lesions performed with perfusion CT. The searches were undertaken in English or Chinese language in Medline, PubMed, Embase, Cochrane Library, Web of Science, and China National Knowledge Infrastructure database from Jan 2010 to Nov 2018. Standardized mean differences (SMDs) and 95% confidence intervals (CIs) of blood volume (BV), blood flow (BF), mean transit time (MTT), and permeability surface (PS) were calculated using Review Manager 5.3. Publication bias, sensitivity, specificity, and the area under the curve (AUC) were calculated using Stata12.0.

Results: Fourteen studies comprising 1032 malignant and 447 benign pulmonary lesions were analyzed. Lung cancer had higher BV, BF, MTT, and PS values than benign lesions. SMDs and 95% CIs of BV, BF, MTT, and PS were 2.29 (1.43, 3.16), 0.50 (0.14, 0.86), 0.55 (0.39, 0.72), and 1.21 (0.87, 1.56), respectively. AUC values of BV and PS were 0.92 (0.90, 0.94) and 0.83 (0.80, 0.86), respectively.

Conclusions: CT perfusion imaging is a valuable technique for the diagnosis of pulmonary nodules. Lung cancer had higher perfusion and permeability than benign lesions. The evidence suggests blood volume is the best surrogate marker for characterizing the blood supply, while permeability surface has a high specificity in quantifying the vascular permeability.

MeSH Keywords: **Blood Volume • Lung Neoplasms • Perfusion Imaging • Permeability • Tomography, X-Ray**

Full-text PDF: <https://www.medscimonit.com/abstract/index/idArt/914206>

 3312

 2

 7

 29



Background

World-wide, lung cancer is the leading cause of cancer deaths; this includes China [1]. Because of the relatively long doubling time of lung cancer cells, an early diagnosis and timely surgical intervention may produce a 5-year survival rate as high as 90%. Because of the aggressive nature of malignant tumors during the growth period, their morphological characteristics and enhancement modes are generally used to make a preliminary diagnosis of the pulmonary nodules in the clinic, and a series of radiomics studies based on texture analysis of pulmonary nodules have received attention for better interpreting the morphological heterogeneity and disordered proliferation of tumor cells than using the traditional CT images [2]. However, these methods cannot provide sufficient functional information for a comprehensive diagnosis of pulmonary nodules. In contrast, multi-slice CT perfusion imaging is an advanced imaging technology which can qualify the hemodynamic changes and provide several perfusion parameters, including blood volume (BV), blood flow (BF), mean transit time (MTT), and permeability surface (PS); this additional information helps clinicians make more accurate diagnoses or management decisions. Pathologically, the blood supply of benign nodules is generally supplied by normal and intact capillaries, whereas capillaries of malignant nodules tend to be immature and highly permeable with incomplete endothelium. The differences of blood supply and permeability between benign and malignant nodules may be assessed using perfusion CT imaging.

With the increasing use of advanced imaging techniques, more studies focusing on the diagnosis of pulmonary nodules using perfusion CT have been published in recent years. However, the findings from these studies are not always in agreement. For instance, most authors believe that malignant nodules have higher BV, BF, and MTT values than benign ones [3–5], whereas Xing et al. [6] reported that BV and MTT levels of malignant lesions are lower than that of benign ones. In contrast to these studies, no significant significance was found for BF and BV levels between malignant and benign nodules [7], MTT levels [8], or MTT and PS levels [9]. In addition, although inflammatory masses are benign lesions, the rich blood supply of inflammatory lesions are not equivalent to that of general benign tumors or chronic granulomatous lesions. We felt it important to explore the perfusion differences between lung cancer and inflammatory mass in a subgroup analysis [10]. As radiation doses have been greatly reduced with the improvement of perfusion algorithms and CT scanners, perfusion imaging has become much more important in the differentiation of pulmonary nodules. The purpose of the present study was to provide a systematic review and meta-analysis with a large sample size to address the contradictory findings from the aforementioned studies, and to evaluate the diagnostic performance of perfusion CT in differentiation of pulmonary

nodules, the results of which may provide more reliable information to clinicians under the current evidence.

Material and Methods

Data sources and search methods

The literature on differential diagnosis of pulmonary lesions using perfusion CT imaging was systematically searched in Medline, PubMed, Embase, Cochrane Library, Web of Science, and China National Knowledge Infrastructure database from Jan 2010 to Nov 2018 independently by 2 reviewers. The languages were limited to English or Chinese. The following keywords were used in the search in either the title or abstract of the article: “pulmonary or lung” and “nodule or mass or lesion” and “perfusion CT or BV or BF or MTT or PS”. We also performed manual retrieval and scrutinized relevant references in the included studies to avoid missing some valuable studies.

Study selection

Two reviewers who were blind to the institutions and journals reviewed the potential studies independently. The inclusion criteria were as follows: (a) perfusion CT was applied in differentiating pulmonary nodule or mass; (b) at least one of the perfusion parameters for BV, BF, MTT, and PS could be extracted or calculated from the original study; (c) tumors must be confirmed by pathology, and inflammatory masses or lesions can be diagnosed by clinical treatment or follow-up; (d) neither medication nor surgery was applied before CT examination; and (e) the scores of quality assessment related to the quality of study design were at least 9 [11,12]. Evaluation criteria are stated in the quality assessment section. The exclusion criteria were as follows: (a) case report, review, letter, meeting record, graduation thesis, or studies not yet published; (b) duplications which originated from the same authors; and (c) MRI or PET perfusion imaging.

Data abstraction and quality assessment

The following items were collected in this analysis: first author, publication year, age, nodule size, nodule number, contrast agent, journal, post-processing software, mean value and standard deviation, and sensitivity and specificity of related parameters. True positive, false positive, false negative, and true negative values were also needed to calculate diagnostic values. We assessed the quality of each study with 14 criteria in terms of the risk of bias using the Revised Quality Assessment of Diagnostic Accuracy Studies (QUADAS-2) checklist [13]. The criteria were judged as “Yes (low risk of bias),” “No (high risk of bias),” or “Unclear.” We discussed or invited a senior clinician to reach a consensus when the results were discordant.

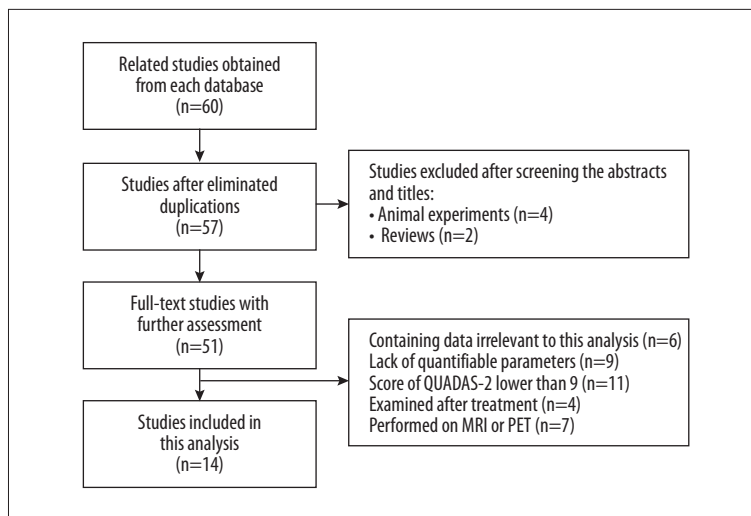


Figure 1. Selection and identification processes based on inclusion and exclusion criteria.

Data synthesis

We calculated the effect size and 95% confidence interval (CI) using Review Manager software version 5.3 (Cochrane Collaboration, Oxford, UK). Publication bias was evaluated by calculating the P value using Stata version 12.0 (StataCorp LP, College Station, TX). $P > 0.05$ of Begg's test denoted no significant publication bias. Inconsistency index and Cochran's Q test were used to estimate inter-study heterogeneity which may originate from age, gender, tumor subtype, flow velocity, and dose, and influence the accuracy of the pooled results; $I^2 > 50\%$ or $P < 0.05$ was considered potential heterogeneity, and a random-effects model was applied for calculating the pooled results. Otherwise, a fixed-effects model was appropriate. As the parameters from different studies varied to some extent, we used the standardized mean difference (SMD) as the pooled results, which suggested less heterogeneity compared to weighted mean difference. Stata.12.0 was used to calculate the pooled sensitivity, specificity, positive likelihood ratio, negative likelihood ratio, diagnostic odds ratio (DOR), area under the curve (AUC), and their 95% CIs with a bivariate mixed-effects binary regression model. The receiver operating characteristic (ROC) curve was used to determine the diagnostic value of BV and PS in distinguishing between lung cancer and benign lesions.

Results

Literature search and selection of studies

We initially retrieved 60 studies by searching the key words in titles and abstracts. Nine studies were excluded; these included animal experiments, duplications of studies by the same authors, and reviews. After downloading and reading full texts of the remaining 51 studies, we excluded an additional 15 studies because of data irrelevant to this analysis or lack of

quantifiable parameters in the related studies. Eleven studies were excluded for the assessment quality scores lower than 9, 4 studies for perfusion imaging was examined after treatment, and 7 studies for the examinations were performed on MRI or PET. Eventually, a total of 14 studies (10 studies in English and 4 studies in Chinese) comprising 1032 malignant and 447 benign nodules were accepted for the analysis. A flowchart detailing the selection process based on inclusion and exclusion criteria is shown in Figure 1. Patient characteristics and imaging protocols of the included studies are summarized in Table 1.

Quantitative analysis

BV for differentiation of pulmonary lesions

The BV values of lung cancer and benign nodules or masses from all studies included in this analysis were compared. Heterogeneity tests indicated significant heterogeneity between studies ($\chi^2=443.61$, $I^2=97\%$, $P < 0.001$). Therefore, we pooled BV using a random-effects model; the pooled SMD of BV was 2.29 (1.43, 3.16), $P < 0.001$ (Figure 2). The Begg's test showed a potential publication bias effect in BV ($P=0.029$).

BF for differentiation of pulmonary lesions

The BF values of lung cancer and benign nodules or masses from 7 included studies were compared. Heterogeneity tests indicated moderate heterogeneity between studies ($\chi^2=23.02$, $I^2=74\%$, $P < 0.001$). Therefore, we pooled BF using a random-effects model; the pooled SMD of BF was 0.50 (0.14, 0.86), $P=0.007$ (Figure 3). The result of Begg's test showed no publication bias effect in BF ($P=0.887$).

Table 1. Characteristics of studies included in the meta-analysis.

Author	Year	Age (years)	Nodule size (mm)	Malignant (n)	Benign (n)	Detector (row)	Contrast type	Flow rate	Dose	Journal	Quality assessment	Post-processing
Ohno et al. [14]	2013	72±10	16.1±8.2	57	39	320	lopromide 300	5 ml/s	0.2 ml/kg	Am J Roentgenol	12	Advanced Body Perfusion
Xing et al. [6]	2009	55.5 (18-90)	NA	58	13	16	lopromide 300	4 ml/s	40 ml	Chinese J Med Imaging	10	CT perfusion 2
Lv et al. [15]	2016	52.4±13.6	NA	350	43	64	lopromide 300	5 ml/s	50 ml	J BUON	11	Body tumor Perfusion software
Hou et al. [5]	2017	62±10	≤30	91	132	NA	lopromide	4 ml/s	40 ml	J Clin Lab Anal	13	CT perfusion software
Sitartchou et al. [9]	2008	63 (38-85)	9-47	51	6	64	lodixanol 270	5 ml/s	50 ml	Invest Radiol	13	CT Perfusion 3
Shan et al. [16]	2012	55 (25-85)	10-30	43	22	64	Vispaue 320	5 ml/s	50 ml	Eur J Radiol	13	CT Perfusion 3
Li et al. [4]	2010	55.7 (24-79)	≤30	46	22	64	lopromide 300	6-7 ml/s	50 ml	Brit J Radiol	12	Brilliance perfusion
Sun et al. [7]	2016	60.8±9.6	18.6 (3-28)	54	17	256	lopamidol 350	4 ml/s	50 ml	Eur J Radiol	13	Syngo Volume Perfusion CT Body
Wang et al. [3]	2017	26-76	NA	21	21	64	lohexol 350	3-4 ml/s	1.5 ml/kg	Biomed Res-India	9	CT perfusion 4.0
Shu et al. [17]	2013	52.8 (28-79)	23 (8-30)	76	32	64	lopromide	5 ml/s	50 ml	Clin Imag	10	CT perfusion 3
Ma et al. [10]	2008	51.27±13.83	28 (16-42)	39	12	16	lopromide 300	4 ml/s	50 ml	BMC Cancer	13	CT Perfusion 3
Xiao et al. [18]	2015	55.63±14.21	≤30	34	12	64	lodixanol 270	4 ml/s	50 ml	Chin Comput Med Imag	10	Perfusion 4-body tumor
Zhang et al. [19]	2005	54.6 (7-82)	20-40	62	26	8	lopromide 300	4 ml/s	50 ml	Chin J Radiol	9	CT perfusion 2
Gu et al. [8]	2013	24-77	NA	50	50	16	loversol 300	4 ml/s	50 ml	Chin J Clin Radiol	11	GE Perfusion 4

NA – not available.

MTT for differentiation of pulmonary lesions

The MTT values of lung cancer and benign nodules or masses from 7 included studies were compared. Heterogeneity tests indicated no heterogeneity between studies ($\chi^2=10.45$, $I^2=43\%$, $P=0.11$). Therefore, we pooled MTT using a fixed-effects model; the pooled SMD of MTT was 0.55 (0.39, 0.72), $P<0.001$ (Figure 4). The result of the Begg’s test showed no publication bias effect in MTT ($P=0.230$).

PS for differentiation of pulmonary lesions

The PS values of lung cancer and benign nodules or masses from 7 studies included in this analysis were compared. Heterogeneity tests indicated mild heterogeneity between studies ($\chi^2=16.61$, $I^2=64\%$, $P=0.01$). Therefore, we pooled MTT using a random-effects model; the pooled SMD of PS was 1.21 (0.87, 1.56), $P<0.001$ (Figure 5). The result of the Begg’s test showed no publication bias effect in PS ($P=0.548$).

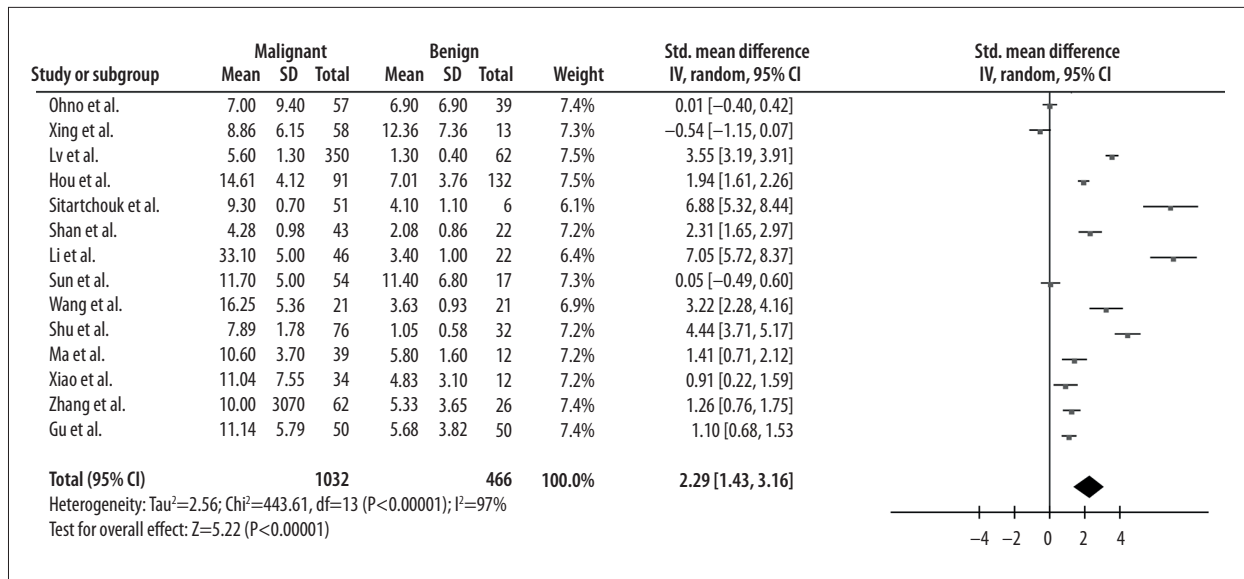


Figure 2. Forest plot of the mean value of blood volume (BV) between lung cancer and benign lesions using a random-effects model (left chart listed by mean BV \pm SD ml/100 g). The CIs of most studies are on the right side of the central axis (x=0), which indicates BV of lung cancer was higher than that of benign lesions.

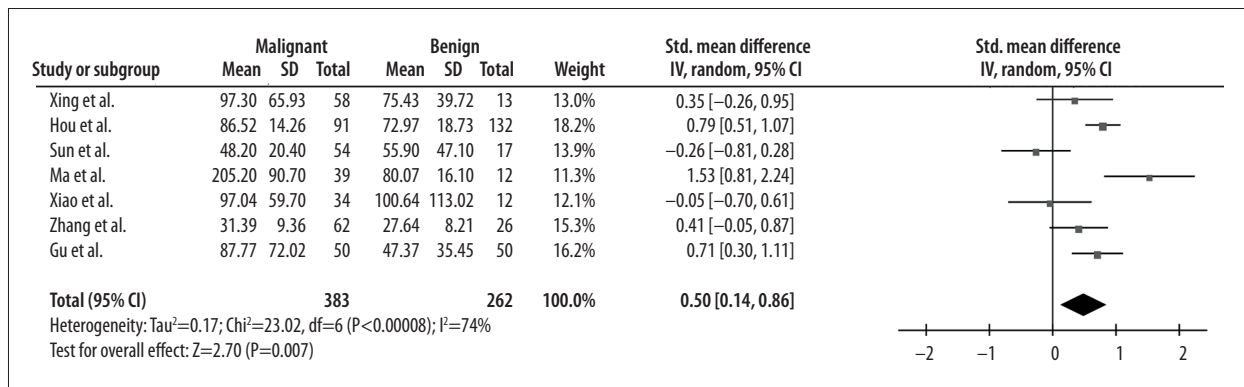


Figure 3. Forest plot of the mean value of blood flow (BF) between lung cancer and benign lesions using a random-effects model (left chart listed by mean BF \pm SD ml/min/100 g). The CIs of most studies are on the right side of the central axis (x=0), which indicates Bf of lung cancer was higher than that of benign lesions.

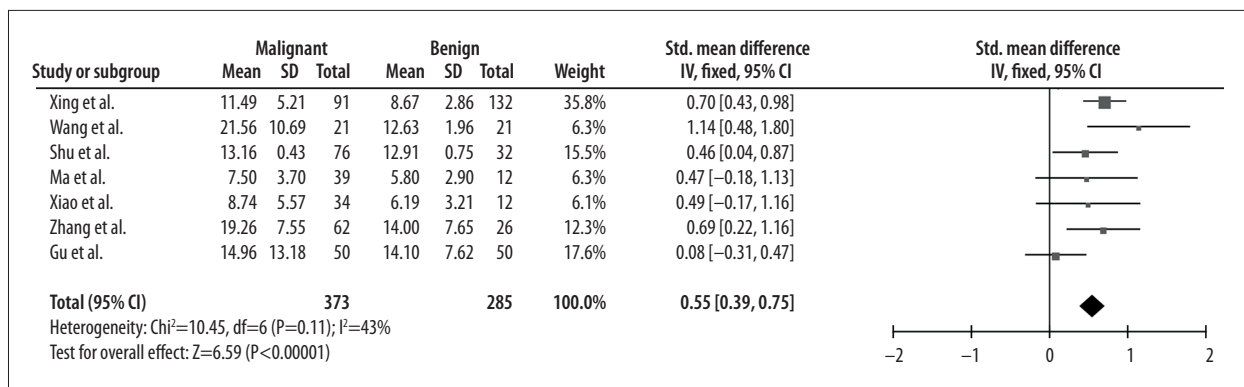


Figure 4. Forest plot of the mean value of mean transit time (MTT) between lung cancer and benign lesions using a fixed-effects model (left chart listed by mean MTT \pm SD sec). The CIs of most studies are on the right side of the central axis (x=0), which indicates MTT of lung cancer was higher than that of benign lesions.

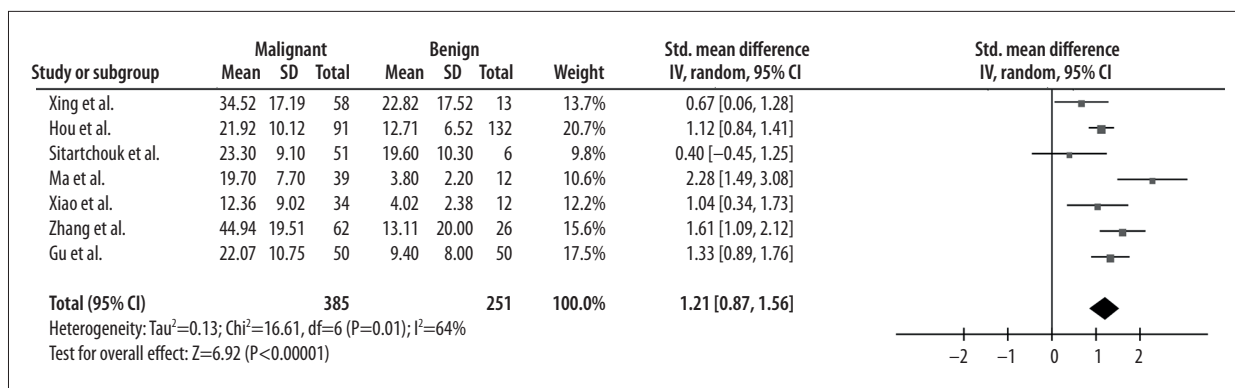


Figure 5. Forest plot of the mean value of permeability surface (PS) between lung cancer and benign lesions using a random-effects model (left chart listed by mean BF ±SD ml/min/100 g). The CIs of most studies are on the right side of the central axis (x=0), which indicates PS of lung cancer was higher than that of benign lesions.

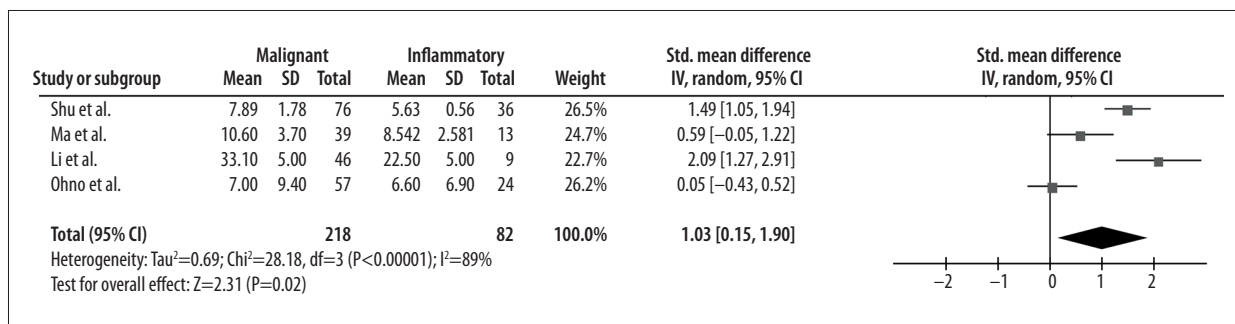


Figure 6. Forest plot of the mean value of blood volume (BV) between lung cancer and inflammatory mass using a random-effects model (left chart listed by mean BV ±SD ml/100 g). The CIs of most studies are on the right side of the central axis (x=0), which indicates Bf of lung cancer was higher than that of inflammatory mass.

Subgroup analysis of BV between lung cancer tumor and inflammatory mass

As mentioned in the introduction, we felt it important to analyze differences not only between benign lesions and malignant tumors, but also between inflammatory lesions and malignant tumors, as both have rich blood supplies. In addition, we used a subgroup analysis to explore the high heterogeneity in BV values. Four related studies concerning the differentiation of malignant tumor from inflammatory masses using BV values were analyzed. The heterogeneity decreased slightly (I² dropped from 97% to 89%). The pooled SMD of BV in the subgroup was 1.03 (0.15, 1.90), P<0.001 (Figure 6).

Diagnosis values of BV and PS

Because of the limited data on the diagnostic efficacy of BF and MTT, we only analyzed the pooled sensitivity, specificity, positive likelihood ratios, negative likelihood ratios, diagnostic odds ratios, and AUCs of BV and PS in this study. The results are shown in Table 2. No obvious threshold effects could be seen in the accuracy estimation of BV and PS (P>0.05). The summary receiver operating characteristic curves are presented in

Figure 7. The sensitivity values for BV and PS showed moderate heterogeneity (I²=78.41%, 88.36%, respectively), and specificity of BV showed mild heterogeneity (I²=67.26%), whereas PS had no obvious heterogeneity (I²=0). Deeks' test, which was mainly applied to the diagnostic meta-analysis, revealed that both BV and PS had no significant publication bias (P=0.764 and P=0.293). The results suggested that BV had higher DOR 34 (16, 72) and AUC values 0.92 (0.90, 0.94) than PS DOR: 28 (12, 63), AUC: 0.83 (0.80, 0.86).

Discussion

CT is the main imaging modality used in the differential diagnosis of pulmonary nodules. Traditionally, it is believed that the degree of enhancement has a close relationship with the grade of malignancy of nodules. Swensen et al. [20] revealed that enhancement less than 15 HU suggests benign neoplasms, and Yamashita et al. [21] reported that enhancement ranging from 20 HU to 60 HU is a reliable indicator for the diagnosis of lung cancer.

Table 2. Diagnosis values of BV and PS.

Index	Combined studies	Sensitivity (95% CI)	Specificity (95% CI)	PLR (95% CI)	NLR (95% CI)	DOR (95% CI)	AUC (95% CI)	I ²	
								Sensitivity	Specificity
BV	9	0.90 (0.84, 0.94)	0.79 (0.67, 0.88)	4.4 (2.7, 7.1)	0.13 (0.08, 0.20)	34 (16, 72)	0.92 (0.90, 0.94)	78.41%	67.26%
PS	5	0.89 (0.77, 0.95)	0.78 (0.70, 0.84)	4.0 (3.0, 5.2)	0.14 (0.07, 0.30)	28 (12, 63)	0.83 (0.80, 0.86)	88.36%	0

BV [4,5,8,9,14,16–19]; PS [5,8,16,18,19]. MTT and BF are not listed because there were not enough studies for diagnostic analysis. BV – blood volume; PS – permeability surface; PLR – positive likelihood ratio; NLR – negative likelihood ratio; DOR – diagnostic odds ratio; AUC – area under the curve; CI – confidence interval.

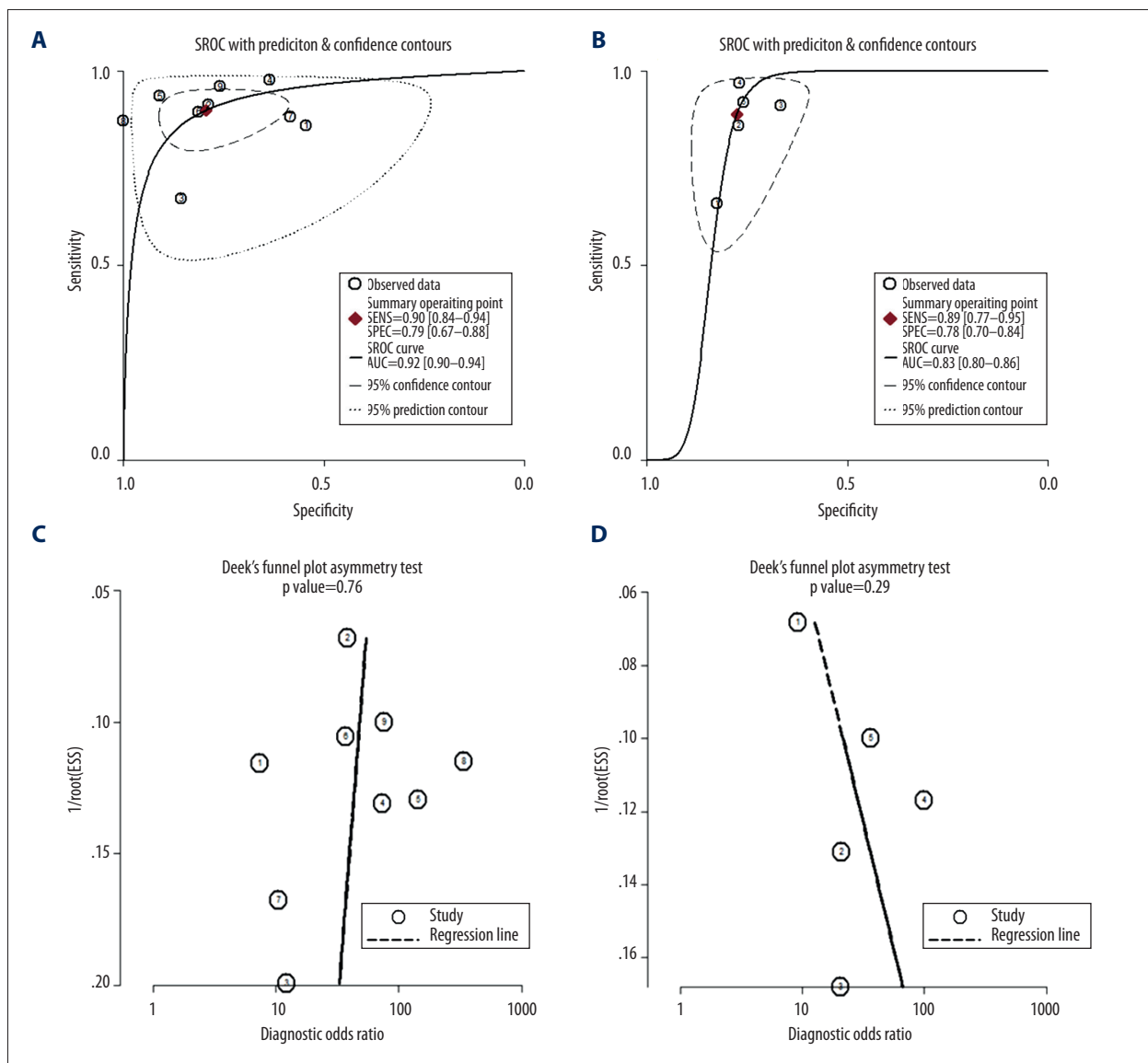


Figure 7. (A, B) Summary receiver operating characteristic curve of blood volume (BV) and permeability surface (PS) in the differentiation of pulmonary nodules. (C, D) Deek's funnel plots of BV and PS. BV reveals a larger AUC than PS. Both funnel plots do not show publication bias.

Clinicians also obtained functional information from dynamic contrast-enhanced imaging, including the type of time density curve (TDC). The shape of the TDC of malignant nodules were obviously different from that of benign ones [10]. TDC of benign nodules mainly displayed a flat trend without a steep slope, while TDC of lung cancer manifested a rapid and steep increase, and changed little after reaching a peak. However, because of relatively low scanning speeds and non-strict time intervals during repeated scanning, the enhancement of the lesion mainly reflected the amount and distribution of the contrast agent deposited in the extravascular space, which could not fully reflect the vascularity and blood supply within the lesions [22].

In recent years, perfusion imaging has been widely used clinically and is able to provide not only morphological characteristics, but also more detailed functional or metabolic information, for the diagnosis and differentiation of pulmonary lesions. In addition, an accurate preoperative differentiation between benign and malignant nodules has been shown to reduce the surgical rates for benign lesions and decrease delay in the removal of malignant tumors [5]. Thus, we undertook this meta-analysis to confirm the diagnostic value of perfusion computed tomography (CT) for distinguishing between malignant and benign pulmonary lesions.

In this meta-analysis, the pooled SMD of BV and BF of lung cancer were higher than those of benign lesions; the results were statistically significant. BV is defined as the volume of blood within the vasculature of tissues and is associated with the diameter and number of open vessels. BF refers to the amount of blood through a section of vessels per unit time, which were closely correlated with the fluency of the draining vein, lymphatic return, and level of BV [5]. Lung cancer is characterized by neovascularization and increased angiogenic activity due to the stimulation of vascular growth factors [23]. The new vessels are the foundation of the growth and metastasis of tumors, and they are generally nourished by luxuriant blood flow originating from the bronchial artery [24]. Ma et al. [10] found that MVD was positively correlated with BF ($r=0.432$, $P=0.019$) and BV ($r=0.429$, $P<0.020$) of peripheral lung cancer in the cases of VEGF positive expression. Li et al. [25] also reported that BV was positively correlated with the extent of MVD in peripheral lung carcinoma ($r=0.761$, $P<0.001$). The composition of benign lesions mainly consisted of tuberculoma, hamartoma, granuloma, inflammatory pseudotumor, and organizing pneumonia, which varied from study to study in this meta-analysis. Few of them showed obvious neovascularization. Relatively low microvessel density (MVD) results in lower vascular supply, and the hemodynamic and pathophysiological differences between lung cancer and benign lesions supported our pooled results in this analysis.

PS is a diffusion coefficient which describes the one-way transmission speed of contrast agents through capillary endothelium. It is strongly correlated with the integrity of endothelial cells and inter-cellular space of the tissues [5]. The new vessels of malignant neoplasms are almost immature, and the structures of vascular walls, including basement membranes and epithelial cells, are incomplete [26]. Coupled with a variety of vascular growth factors, the permeability of capillaries increase and facilitate the transmission of contrast agent into the interstitial space. This behavior provides an explanation for the higher PS levels in lung cancer than those of benign lesions, in our meta-analysis.

This analysis revealed that lung cancer has higher MTT than benign lesions. MTT refers to the transit time of the contrast agent through the micro-circulation. Except for the characteristics mentioned above, the interstitial space of lung cancer was found to be larger, and a near absence or substantial reduction of lymphatic vessel was noted [10]. In addition, the newly-formed tumor vessels were tortuous, and the diameters differed in sizes. All these factors contributed to the retention of contrast agents within the interstitial space, and a longer transit time was found. Similarly, Ma et al. [10] reported that peripheral lung cancer maintains a relatively long plateau after reaching a peak using TDC in a dynamic enhanced CT imaging, compared to benign nodules, whose TDC changed little, with a nearly flat trend.

Our subgroup analysis revealed that the BV of lung cancer was higher than that of inflammatory masses, with statistical significance. However, in the relevant studies (using spectral CT imaging) of Lin et al. [27] and Wang et al. [28], higher iodine concentrations (IC) and normal iodine concentrations (NIC), which can reflect the blood supply of the lesions, were found in active inflammatory nodules but not in lung cancer. These results contradicted our subgroup analysis. Firstly, the blood supply of acute inflammatory masses or granulomas was also abundant in the effect of inflammatory factors, which led to a high IC in the lesions. Secondly, the IC was also closely correlated with the flow rate of injection, dose of contrast agent, and extraction of iodine from micro-circulation [27]. Thirdly, the included cases of inflammatory lesions varied considerably between studies. These inconsistencies reduce the reliability of the results. Lastly, there were not enough studies on the differentiation of inflammatory lesions and lung cancer for statistical quantification. The results remained unclear, which promises a meaningful research direction in larger prospective studies to address the issue of blood supply.

In contrast, inflammatory masses were generally characterized by dilation and congestion of vasculature rather than neovascularization in the early stages. Mature capillaries contain intact basement membrane and continuous endothelial cells.

As a result, the permeability of benign lesions including inflammatory masses, quantified by PS, should be low. In addition, high interstitial pressure resulting from tissue edema and congestion slows down the transmission and decreases PS. Both studies of Shu et al. [17] and Ma et al. [10] showed that PS of lung cancer was higher than that of inflammatory and benign nodules, which suggests that PS may be a highly specific parameter for differentiating lung cancer from inflammatory lesions on the basis of vascular permeability.

The heterogeneity analysis was an indispensable consideration of this meta-analysis. Although we set strict inclusion and exclusion criteria for including the same objective and high-quality studies, BV, BF, and PS still showed moderate and greater heterogeneity. There were some potential confounding factors, which may have reduced the homogeneity of the included studies. Firstly, the nodule sizes ranged from 9 to 42 mm in diameter. The sizes of nodules, especially in those malignant tumors, may indicate different growth periods. This indicates that the demand for blood supply and degree of neovascularization may not have been equal, which may have led to ambiguous results. Secondly, many perfusion algorithms have been developed and applied to in-house or commercial software for post-processing of clinical samples. Goh et al. [29] compared 2 commercially available perfusion software packages and found there were inconsistencies between the 2 methods used to evaluate tumor vascularity, which revealed that the measurement techniques were not directly interchangeable. Thirdly (as previously mentioned), although lung cancer and benign lesions were investigated, the characteristics of included cases differed to a large extent, especially benign lesions, which may be confounded with some high perfusion cases (e.g., pneumonia, abscess and acute inflammatory masses). The heterogeneity of BV was decreased in a subgroup analysis. Lastly, some potential factors such as scanning method, application of multi-slice spiral CT, cardiac output, contrast agents, radiation dose, reconstruction algorithms (smooth vs. sharp), slice thickness, and other factors listed in Table 1 could also have introduced heterogeneity in our study. Although some of the results from different studies

were diametrically opposed, with high heterogeneity, both conflicting and negative studies were included in this meta-analysis and the publication bias was insignificant, as we expected. The diagnostic thresholds of all the parameters were inconsistent among the included studies, but we found no threshold effect-related heterogeneity after performing heterogeneity tests, which means the merged results are credible.

There are some limitations to this meta-analysis. Most of the studies we included were performed in China, which may limit the applicability of this study to other countries. In addition, the number of studies concerning the differentiation between lung cancer and inflammatory masses with PS, MTT, or BF was not large enough to perform a subgroup analysis. Future researched with larger sample sizes, consistent imaging protocols, and a greater homogeneity of patient demographics are needed to establish credible diagnostic thresholds in the future. Finally, relevant perfusion studies performed in MRI or PET were not compared in this meta-analysis. The feasibility of widespread use of CT perfusion imaging for distinguishing between lung cancer and benign lesions needs further investigation.

Conclusions

CT perfusion imaging is a valuable technique for the analysis of pulmonary nodules and may reflect the level of tumor angiogenesis *in vivo* on a molecular level. Besides, the pooled evidence suggest that lung cancer had higher perfusion and permeability than benign lesions, and BV is the best parameter for characterizing the blood supply of lung tumors, whereas PS has a high specificity for quantifying the permeability of vascularity. Although shortcomings exist in CT imaging methodologies, future in-depth investigations on low-dose perfusion imaging methods will likely lead to improved differentiation of pulmonary nodules.

Conflicts of interest

None.

References:

1. Siegel RL, Miller KD, Jemal A: Cancer statistics, 2017. *Cancer J Clin*, 2017; 67(1): 7–30
2. Zhao Q, Shi CZ, Luo LP: Role of the texture features of images in the diagnosis of solitary pulmonary nodules in different sizes. *Chinese J Cancer Res*, 2014; 26(4): 451–58
3. Wang G, Zhou XM, Zhao RR et al: Multi-slice spiral computed tomography perfusion imaging technology differentiates benign and malignant solitary pulmonary nodules. *Biomed Res-India*, 2017; 28(10): 4605–9
4. Li Y, Yang ZG, Chen TW et al: First-pass perfusion imaging of solitary pulmonary nodules with 64-detector row CT: Comparison of perfusion parameters of malignant and benign lesions. *Brit J Radiol*, 2010; 83(993): 785–90
5. Hou H, Xu Z, Zhang H, Xu Y: Combination diagnosis of multi-slice spiral computed tomography and secretory phospholipase A2-IIa for solitary pulmonary nodules. *J Clin Lab Anal*, 2018; 32(2)
6. Xing N, Cai ZL, Zhao SH, Yang L: [The comparative study of CT perfusion parameters of solitary pulmonary nodules with microvessel density.] *Chinese J Med Imaging*, 2009; 19(4): 251–54 [in Chinese]
7. Sun YB, Yang MJ, Mao DB et al: Low-dose volume perfusion computed tomography (VPCT) for diagnosis of solitary pulmonary nodules. *Eur J Radiol*, 2016; 85(6): 1208–18
8. Gu Y, Zhou SL, Yuan G, Huang LQ: [The evaluation of CT perfusion, routine and computer aided diagnosis of solitary pulmonary occupation.] *Chin J Clin Radiol*, 2013; 32(7): 963–67 [in Chinese]

9. Sitartchouk I, Roberts HC, Pereira AM et al: Computed tomography perfusion using first pass methods for lung nodule characterization. *Invest Radiol*, 2008; 43(6): 349–58
10. Ma SH, Le HB, Jia BH et al: Peripheral pulmonary nodules: Relationship between multi-slice spiral CT perfusion imaging and tumor angiogenesis and VEGF expression. *BMC Cancer*. 2008; 8: 186
11. Li B, Li Q, Chen C et al: A systematic review and meta-analysis of the accuracy of diffusion-weighted MRI in the detection of malignant pulmonary nodules and masses. *Acad Radiol*, 2014; 21(1): 21–29
12. Wu LM, Xu JR, Hua J et al: Can diffusion-weighted imaging be used as a reliable sequence in the detection of malignant pulmonary nodules and masses? *Magn Reson Imaging*, 2013; 31(2): 235–46
13. Whiting PF, Rutjes AW, Westwood ME et al: QUADAS-2: A revised tool for the quality assessment of diagnostic accuracy studies. *Ann Intern Med*, 2011; 155(8): 529–36
14. Ohno Y, Nishio M, Koyama H et al: Comparison of quantitatively analyzed dynamic area-detector CT using various mathematic methods with FDG PET/CT in management of solitary pulmonary nodules. *Am J Roentgenol*, 2013; 200(6): W593–602
15. Lv Y, Jin Y, Xu D et al: Assessment of 64-slice spiral computed tomography with perfusion weighted imaging in the early diagnosis of ground-glass opacity lung cancer. *J BUON*, 2016; 21(4): 954–57
16. Shan F, Zhang ZY, Xing W et al: Differentiation between malignant and benign solitary pulmonary nodules: Use of volume first-pass perfusion and combined with routine computed tomography. *Eur J Radiol*, 2012; 81(11): 3598–605
17. Shu SJ, Liu BL, Jiang HJ: Optimization of the scanning technique and diagnosis of pulmonary nodules with first-pass 64-detector-row perfusion VCT. *Clin Imag*, 2013; 37(2): 256–64
18. Xiao HJ, Liu YH, Tan HN et al: [Comparative study on low-dose CT perfusion and dynamic contrast-enhanced CT imaging of solitary pulmonary nodule.] *Chin Comput Med Imag*, 2015; 21(1): 30–33 [in Chinese]
19. Zhang JE: [Utility of CT perfusion in pulmonary nodules]. *Chin J Radiol*, 2005; 39(10): 1041–45 [in Chinese]
20. Swensen SJ, Brown LR, Colby TV et al: Lung nodule enhancement at CT: Prospective findings. *Radiology*, 1996; 201(2): 447–55
21. Yamashita K, Matsunobe S, Tsuda T et al: Solitary pulmonary nodule: Preliminary study of evaluation with incremental dynamic CT. *Radiology*, 1995; 194(2): 399–405
22. Ohno Y, Nishio M, Koyama H et al: Dynamic contrast-enhanced CT and MRI for pulmonary nodule assessment. *Am J Roentgenol*, 2014; 202(3): 515–29
23. Yi CA, Lee KS, Kim EA et al: Solitary pulmonary nodules: Dynamic enhanced multi-detector row CT study and comparison with vascular endothelial growth factor and microvessel density. *Radiology*, 2004; 233(1): 191–99
24. Yuan XD, Zhang J, Quan CB et al: Differentiation of malignant and benign pulmonary nodules with first-pass dual-input perfusion CT. *Eur Radiol*, 2013; 23(9): 2469–74
25. Li Y, Yang ZG, Chen TW et al: Peripheral lung carcinoma: Correlation of angiogenesis and first-pass perfusion parameters of 64-detector row CT. *Lung Cancer*, 2008; 61(1): 44–53
26. Xiong Z, Liu JK, Hu CP et al: Role of immature microvessels in assessing the relationship between CT perfusion characteristics and differentiation grade in lung cancer. *Arch Med Res*, 2010; 41(8): 611–17
27. Lin JZ, Zhang L, Zhang CY et al: Application of gemstone spectral computed tomography imaging in the characterization of solitary pulmonary nodules: Preliminary result. *J Comput Assist Tomogr*, 2016; 40(6): 907–11
28. Wang G, Zhang C, Li M et al: Preliminary application of high-definition computed tomographic gemstone spectral imaging in lung cancer. *J Comput Assist Tomogr*, 2014; 38(1): 77–81
29. Goh V, Halligan S, Bartram CI: Quantitative tumor perfusion assessment with multidetector CT: are measurements from two commercial software packages interchangeable? *Radiology*, 2007; 242(3): 777–82